Journal of Materials Processing Tech. 252 (2018) 652–658

Contents lists available at ScienceDirect

Journal of Materials Processing Tech.

journal homepage: www.elsevier.com/locate/jmatprotec

De-agglomeration rate of silicate bonded sand cores during core removal

Bernhard J. Stauder[a,*], Harald Harmuth[b], Peter Schumacher[b]

[a] Nemak Linz GmbH, A-4030 Linz, Austria
[b] Montanuniversitaet Leoben, A-8700 Leoben, Austria

ARTICLE INFO

Keywords:
Casting
Foundry sand core
Core removal
Particle size
Testing

ABSTRACT

The here presented criterion describes the disintegration kinetics of cast in sand cores, which is influenced by transient thermal and mechanical casting process loads.

A semi-permanent mould setup allowing for various thermal exposure intensities was developed and used with wedge shaped, hot hardened silicate bonded sand cores. During defined mechanical agitation of such produced castings the minimum core removal mass rate was identified and combined with the de-agglomeration degree of the collected core sand. The de-agglomeration degree was evaluated from particle size analysis with specifically adapted sieving parameters and a modelling approach for the size distribution. The retained mass on the top mesh constituted the lump mass.

Cast-in cores generally exhibited higher de-agglomeration rates compared to non-cast-in reference cores, which confirmed a deteriorating influence of a casting process on the sand core. Increased de-agglomeration rates and more disintegrated core lumps were observed for the samples with longer thermal exposure. Avoiding ambient humidity resulted in a significantly increased de-agglomeration rate compared to openly stored samples.

1. Introduction

Sand cores are used in numerous metal casting technologies to shape complex internal contours and undercut sections. After the solidification and cooling of a casting, a sand core removal process is required to obtain a sand-free casting. Czerwinski et al. (2015) recently reviewed the state of the art in sand core technology. Over the past century, demands by the automotive casting industry for higher productivity and complex cores have led to the replacement of inorganic binders with organic binders. Due to of more restrictive health and safety guidelines and emissions regulations, inorganic core production technologies are once again being implemented, because these technologies are odourless and nearly emission free. According to Izdebska-Szanda et al. (2012) thermal degradation during casting affects core removal less in inorganic bonded cores than in organic binder systems. Therefore, applying inorganic core binder systems requires special attention to core removal properties.

Gamisch (2002) reviewed existing industrial solutions for core removal. Mechanical core removal processes usually consist of hammering and shaking steps. Fig. 1 shows a typical setup applied for an aluminium cylinder head with inorganically bonded sand cores.

Quantitative evaluation methods for core removal properties are rarely available. Henry (Ashland) et al. (1999) studied the shake-out behaviour of wedge shaped Coldbox test cores cast in aluminium. Using a pressure-controlled pneumatic hammer, they documented the shaken-out sand mass at specific times and the required shake-out time for complete sand core removal. According to them, binder properties influenced core removal more than casting process variations. To transfer their method to foundry applications, they recommended customising a trial setup for given process conditions. Fennell and Crandell (2008) used a similar setup with an in-line scale for sand collection, and evaluated the average shake-out mass rates of different inorganically and organically bonded sand core types. Inorganically bonded samples had a higher shake-out mass rate than organically bonded cores.

At the Polish Foundry Institute, several investigations have been performed using knock-out testing, according to standard (PN-85/H-11005, 1985). In such tests, strokes with a defined energy are placed directly onto a cast-in test core. Izdebska-Szanda et al. (2012) presented the residual strengths of different binders after thermal exposure and using parallel knock out tests. Different organically and inorganically bonded samples were cast in copper and aluminium. The knock-out work remained similar, in contrast with the different retained strength levels after pre-conditioning to equivalent temperature exposures. Subsequent investigations by Major-Gabryś et al. (2014) demonstrated that retained strength measurements could not be used as the criterion for the knock-out properties of silicate bonded cores, once a secondary

* Corresponding author.
E-mail address: bernhard.stauder@nemak.com (B.J. Stauder).

http://dx.doi.org/10.1016/j.jmatprotec.2017.10.027
Received 3 July 2017; Received in revised form 15 October 2017; Accepted 16 October 2017
Available online 19 October 2017

a *b*

Fig. 1. Cylinder head with inorganic test cores during (a) hammering process and (b) shaking process (Nemak, 2005).

hardening maximum above 600 °C was attained. The authors postulated a high degree of mechanical interaction by casting contraction counteracting the expansion of the cast-in core. They proposed high temperature thermal expansion as a more significant criterion for predicting knock-out properties.

In the present study, the kinetics of sand core de-agglomeration are investigated; no contributions to such research could be found in the available literature. Therefore, the field of mineral processing has been evaluated in greater depth, as the fragmentation properties (e.g. of ores or rocks) are central to this field. Rosin and Rammler (1933) developed a basis for investigating coal dust particle size distributions. Based on their work, the Rosin-Rammler-Sperling-Bennet (RRSB) approach was used to describe the particle sizes of dusts, soils, and crushed materials. Note that the RRSB approach represents a specific case of the later-established, widely known Weibull probability distribution (Weibull, 1951). This was applied by Paluszny et al. (2016) to describe the particle size distributions of crushed rocks. Bayat et al. (2015) reviewed the fitting accuracy of several particle size distributions. The physical evidence of various functional approaches for describing particle size distributions was demonstrated by Brown and Wohletz (1995).

In summary, the RRSB approach is widely accepted, and is generally documented in mineral processing handbooks (Fuerstenau and Han, 2003; Zogg, 1993). It is a convenient and approved approach for describing de-agglomeration process results. In this study, this approach will be applied for the first time to a foundry application, to model the achieved particle size distributions of raw sand and removed core sand.

2. Material and methods

Sample production for core removal trials are presented. These include the different applied cooling conditions, the core removal setup, and the particle size evaluation method.

2.1. Test casting production

Silica sand H32 (Quarzwerke, 2009) bonded with 2,5% mass of sodium silicate binder with a molar SiO_2:Na_2O ratio of 325 was used. The sand cores were produced using an electrically heated core box on a Roeper H1 core blowing machine. The cores were hardened in the core box at 160 °C for 2 min, followed by drying in a 120 °C chamber furnace for 5 min. After cooling, the sand cores were sealed in foil to avoid air exchange and intensive humidity condensation during storage.

For casting the test core was placed in a steel mould and liquid Al (alloy AlSi7Cu0,5Mg) at a temperature of 745 ± 10 °C was poured in. Fig. 2 illustrates (a) the schematic mould setup, (b) the test core dimensions, and (c) the core.

The steel mould was operated based on the mould side wall temperature T_M according to Fig. 2a. The mould temperature at the start of pouring was 400 °C. After T_M exceeded its maximum, the casting was gently demoulded at 450 °C. Overall, a cycle time of approximately 7 min was obtained.

Four different thermal exposure scenarios were defined. The following colour coding applies throughout the text and figures:

Hardened reference: non cast-in cores, realised by re-filling the empty cavities of test castings with virgin core sand mixture hardened therein (yellow).

a. Water cooling: realised by setting the casting with the feeder 40 mm deep into a water bath of 60 − 70 °C (blue).
b. Air cooling: cooling the cast samples at non-agitated air ambience (green).
c. Insulation: completely embedding the cast part between 30 mm thick ceramic fibre mats (red).

Table 1 summarises the evaluated thermal exposure time for the casting and cast-in cores, and the time and value of the achieved sand core peak temperatures after the start of pouring. It is not applicable for the hardened reference sample.

Times of thermal exposure of the sand cores are significantly different with the different cooling types. Because the sand cores have low thermal conductivity, they show long heating delays relative to the short pouring time of < 10 s. For the water-cooled case, the sand cores reach their peak temperature even after the casting has been cooled by water quenching. For air and insulation cooled cases, the cooling of the cores is fully linked to that of the castings.

2.2. Core removal trials

A vibration unit equipped with two electrical imbalance drives rotating at 50 Hz has been used for the shake-out trials. The shaken-out sand was directly funnelled onto a balance, and the removed sand mass was recorded with 1 Hz resolution. The test castings were clamped into a vertically guided sample holder, which is shown in Fig. 3.

On top of the sample, a knocking mass has been placed. Both the sample and mass are freely movable in the vertical direction. The maximum vertical acceleration of the vibration unit was measured as 6 *g*. On the sample, a maximum vertical acceleration was measured as 40 *g* for 99 % of the values, with peaks of up to 100 g.

2.3. Particle size analyses

A Retsch AS200 digit sieve machine with meshes of 0 (tray), 63, 90, 125, 180, 250, 355, 500, 710, 1000 and 1400 µm width was used for the particle size analysis, according to the standard sieving procedure (ISO, 2016).

The removed core sand from castings also contains larger agglomerates and core lumps. To avoid their excessive breakdown during sieve analysis, the sieving amplitude was reduced from 1,5 to 0,2 mm, and

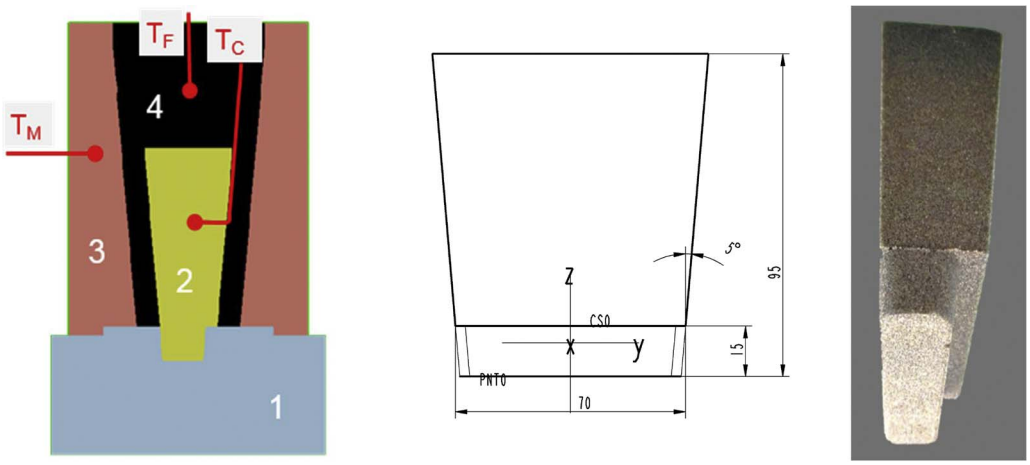

Fig. 2. Test core geometry and mould setup. (a): Schematic cross section through the mould setup consisting of (1) a base plate, (2) a core, and (3) the upper mould part. The casting is formed in the cavity (4). The thermocouple positions are: T_M in the mould, T_C in the core centre, and T_F in the feeder centre. (b): Test core main dimensions and (c) realised core.

Table 1
Main thermal characteristics of test castings and cast-in cores.

Condition	Casting cooling time below 120 °C in s	Sand core exposure time above 120 °C in s	Sand core peak temperature time in s	Sand core peak temperature in °C
Water	400	900	480	380
Air	4000	4000	700	400
Insulation	40000	40000	900	410

the sieving time was reduced from 600 to 60 s. The whole retained sand portion for the largest mesh (1,4 mm) was defined as the lump mass fraction m_l.

3. Results and discussion

3.1. Core removal experiments

Curves for removed mass over time (obtained from the vibration test bench) are presented for the different sample conditions, followed by mass rate and particle size evaluations.

Fig. 4 illustrates the typical visual appearance of the collected removed core sand. The hardened sample yielded finely de-agglomerated sand and a large single core lump. The water −cooled sample revealed very few and small core lumps. In contrast, the air and insulation cooled samples exhibited a significantly higher number of core lumps. Higher initial damage was observed for longer thermal exposure times.

Fig. 5 shows mass curves over time for the four different thermal exposure scenarios. The curve sections with the lowest mass-over-time incline are indicated. The removed core mass curves all have a characteristic shape. An initial transient phase is followed by a steady state phase with a typically lower mass rate; this reflects the maximum sand core resistance. At the end of the process, a final transient phase is observed, where most of the removed sand core is yielded as lumps. Core removal at the end of the process is dominated by the casting geometry and controlled by the size of the opening of the casting. The required time for core removal was typically 5–20 min for the hardened and water-cooled variants and 1–2 min for the air and insulation cooled variants.

To improve manual minimum mass rate evaluation, an objective criterion is required. The minimum core removal mass rate R_{min} can best be described by the quarter mass rate R_{25}, which can be defined as the longest time segment t_Q on a mass-time curve for obtaining 25 % of the total removed core mass m_{tot} (Eq. (1)):

$$R_{25} = \frac{m_{tot}}{4 \cdot t_Q} \tag{1}$$

Fig. 6 illustrates such identified R_{25}-segments for one example of each sample condition. Fig. 7 shows the high correlation between the manually obtained minimum mass rate and R_{25}-criterion. Fig. 8 summarises the obtained quarter mass rate results.

From Fig. 8, it is clear that thermal exposure leads to an increased core removal rate for silicate bonded samples. The slowest core removal was observed for the hardened condition. The water-cooled condition exhibited a 2–3 times larger core removal rate. Significantly higher core removal rates were found for the air and insulation cooled conditions. In particular, the air-cooled condition revealed high scatter, which required deeper investigations into process sensitivity and storage conditions.

In this study, three castings were sealed against air exchange during the cooling phase at a still-elevated casting temperature. This was done to eliminate humidity condensation. For a direct comparison, two more castings were openly stored in ambient air. After 10 h of overnight

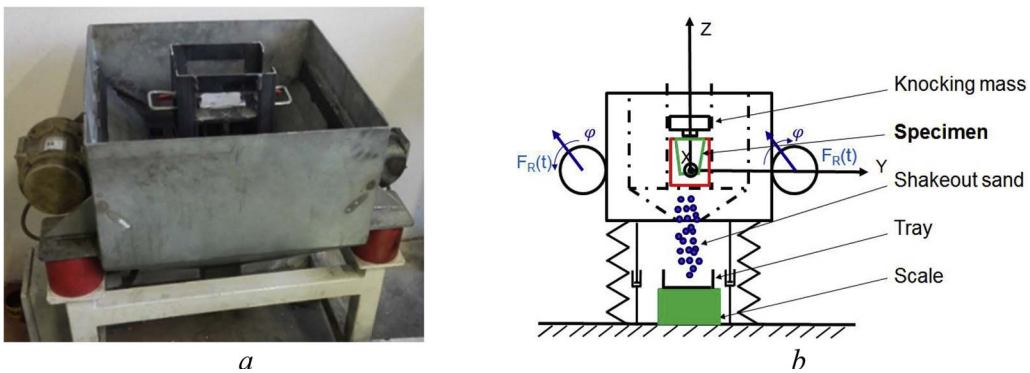

Fig. 3. Vibration unit for shake-out trials. (a) Setup, and (b) Schematic view of the functional elements. The cross section of the hopper opening is 0,8 × 0,8 m^2.

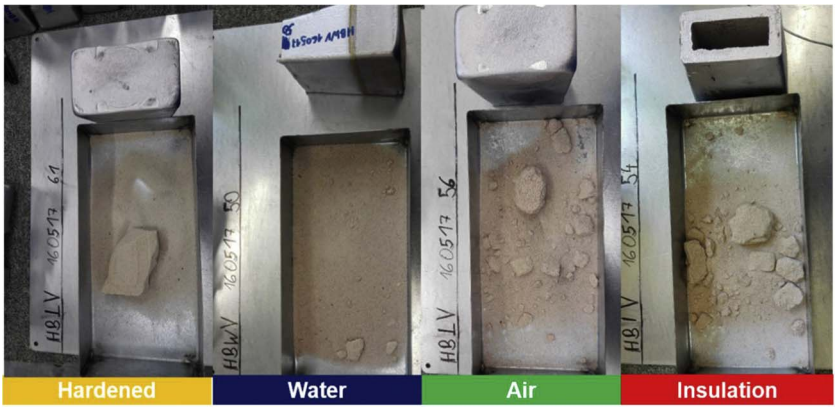

Fig. 4. Results of core removal trials for silicate bonded sand core samples with different thermal exposure conditions. The empty castings are positioned beside the core sand tray.

storage at 25 °C and a relative humidity of 40–50 %, the cores were removed. The resulting mass over time curves are shown in Fig. 9.

The results demonstrate a significant deceleration in core removal for the unsealed samples compared to the sealed samples. The core removal mass-time curves for the unsealed samples are similar to the initial curves presented in Fig. 5(c) and (d). In contrast, the sealed samples had both low scatter and the shortest measured core removal times of all studies.

The silicate bonded sand cores had a propensity to absorb humidity. This prolongs the core removal rate, which is potentially overlaid to all results.

3.2. Particle size evaluation

This section presents an analysis of particle size modelling, and the deduction of the de-agglomeration degree and rate. The achieved results for the different conditions are summarised and discussed.

To apply an extended analysis of the obtained sieve fraction after core removal, a particle analysis according to the RRSB approach was performed. The RRSB function of the retained mass portion R_{RRSB} of the total mass for a particle diameter d_p is shown by Eq. (2).

$$R_{RRSB} = e^{-\left(\frac{d_p}{d'_p}\right)^k} \tag{2}$$

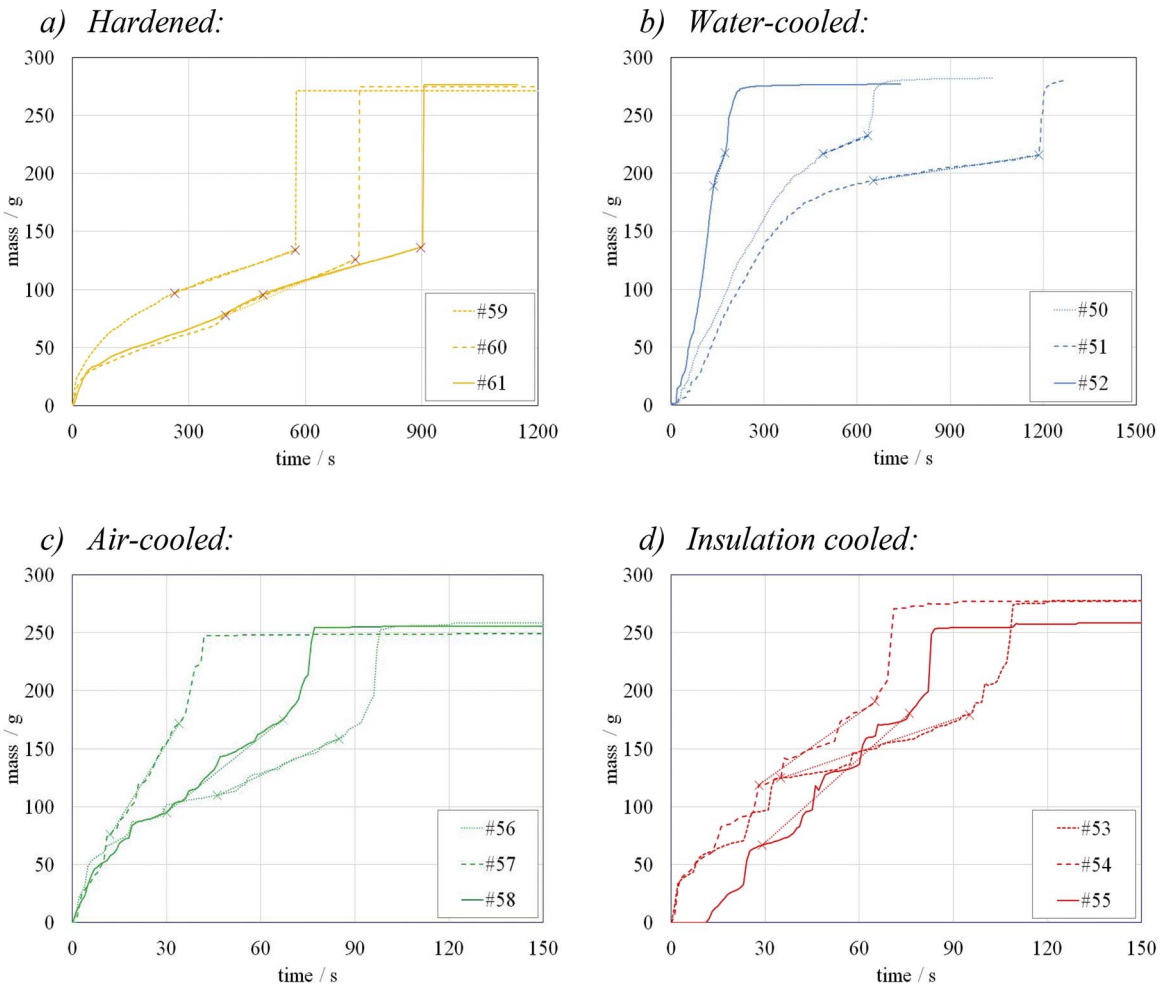

Fig. 5. Mass over time curves for the differently treated samples (# given in Table 3). The manually identified steady state range showing a minimum slope is indicated by X to X.

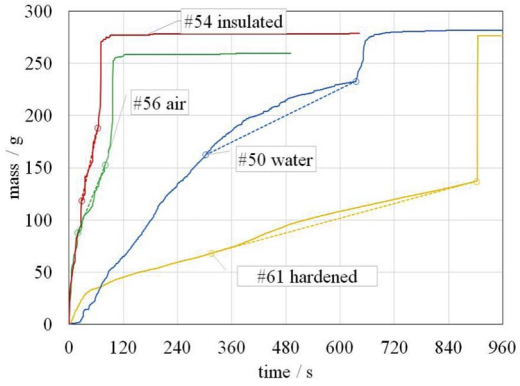

Fig. 6. Typical shake-out mass increase curves for silica bonded samples. One example of every cooling condition including the quarter mass evaluation range is shown.

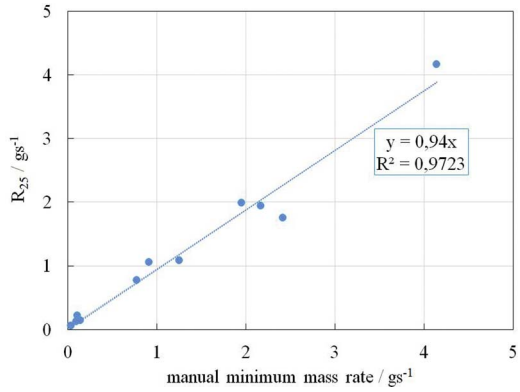

Fig. 7. Correlation of manually evaluated minimum mass rate with quarter mass shake-out rate R_{25}.

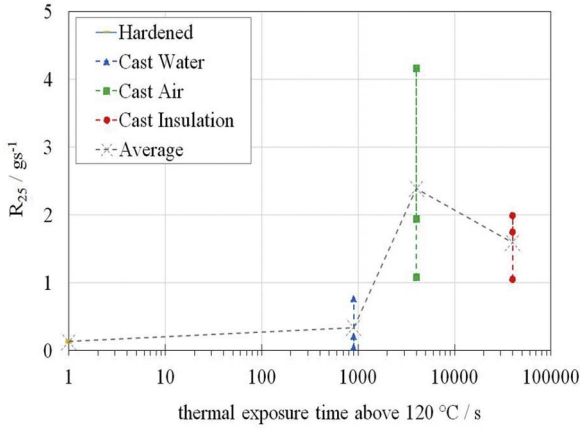

Fig. 8. Minimum core removal mass rate, defined by quarter mass rate. Single measurement results and group average results are shown over thermal exposure time.

k: distribution parameter; d'_p: grain size parameter.

$$s^2 = \frac{\sum_{i=1}^{n} (R_m^i - R_{RRSB}^i)^2}{n-1} \tag{3}$$

During experimental evaluation, the RRSB parameters are obtained by minimising the variance of s^2 the modelled versus the measured particle size distribution curves (Eq. (3)).R_m^i: measured retained mass fraction on mesh i, R_{RRSB}^i: RRSB-modelled retained mass fraction on mesh i

The relevant retained mass fractions for the RRSB fit are those on $n = 9$ meshes from 63 to 1000 µm. Excluded are the collecting tray, which always contains 100 %, and the 1400 µm mesh, which by definition contains m_L. The parameters were fitted with three-digit accuracy.

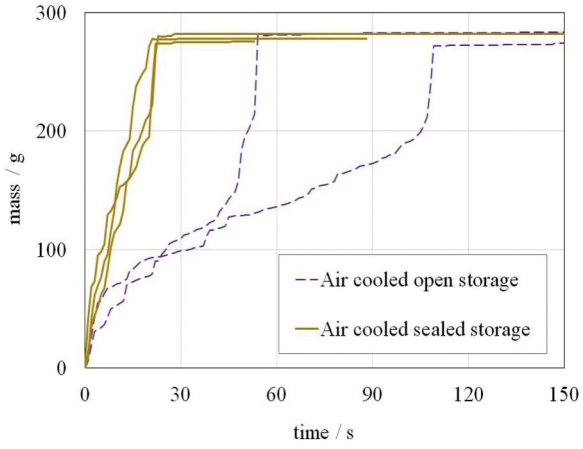

Fig. 9. Mass over time curves of silicate bonded cores with dry storage (solid line) and open storage in ambient air (dashed line).

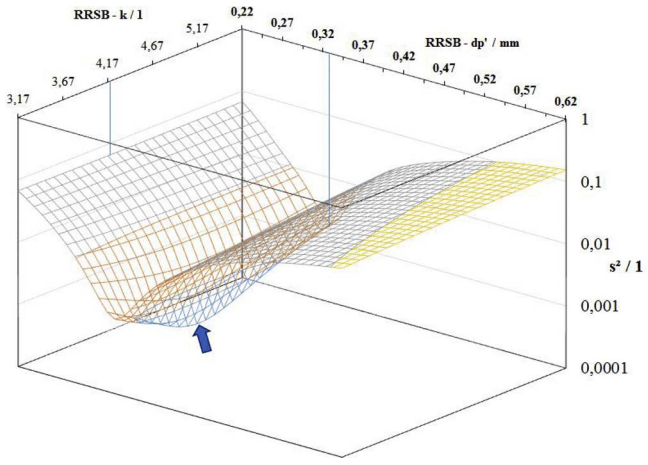

Fig. 10. Variance in RRSB fit for silica raw sand over RRSB-parameters showing a distinct minimum, indicated by the arrow.

Table 2
Sieve analysis of the used silica sand. Lower and upper meshes, measured mass fractions, and the RRSB-modelled retained mass fractions are listed.

Lower mesh in µm	Upper mesh in µm	Sieved mass fraction in %	Retained mass fraction R_m in %	RRSB modelled mass fraction R_{RRSB} in %
0	63	0	100	99,9
63	90	0	100	99,6
90	125	0,3	99,7	98,3
125	180	4,9	94,8	92,5
180	250	22,9	71,9	73,4
250	355	45,4	26,4	26,2
355	500	22,5	3,9	0,4
500	710	3,6	0,3	0
710	1000	0,3	0	0
1000	1400	0	0	0
1400		0	0	0

Assuming spherical particles, the specific surface S_M^{RRSB} can be approximated with an error below 2,5 %, as documented by Eq. (4) (Zogg, 1993).

$$S_M{}^{RRSB} = \frac{A_K}{\rho \cdot V} = \frac{6{,}39}{\rho \cdot d'_p} \cdot e^{\left(\frac{1{,}795}{k^2}\right)} \tag{4}$$

A_K: granulate surface; ρ: density; V: volume.

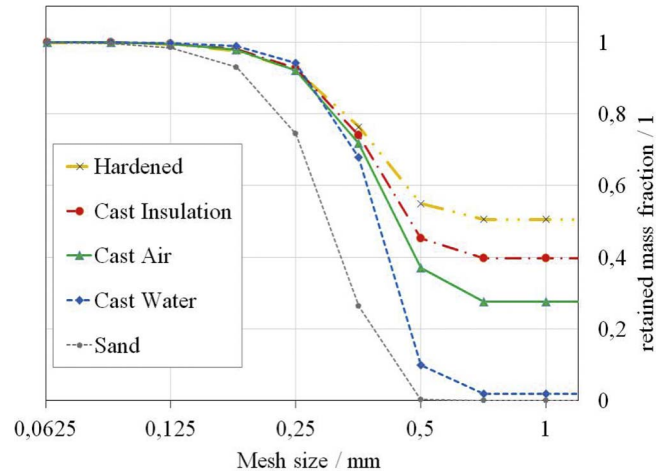

Fig. 11. Retained mass fraction from sieve analysis for removed core sand from all thermal exposure conditions compared to the raw sand.

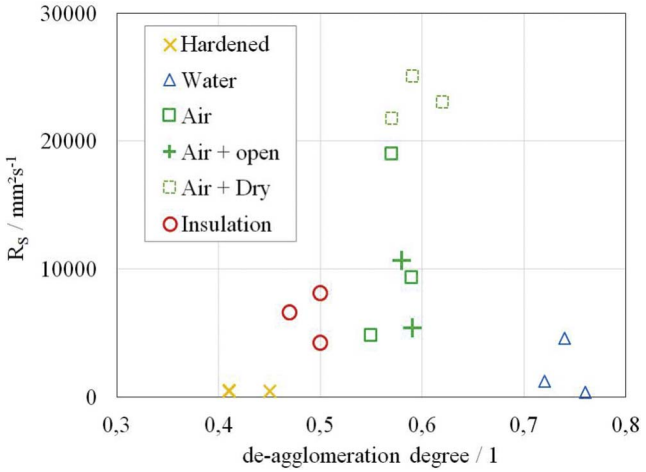

Fig. 12. De-agglomeration rate over de-agglomeration degree for different investigated thermal exposure conditions of investigated sand cores.

Because of its low specific surface contribution, the lump mass fraction will be excluded from the specific surface evaluation of core sand S_M^{sand}, leading to Eq. (5):

$$S_M^{coresand} = S_M^{RRSB}.(1 - m_L) \quad (5)$$

The researched de-agglomeration degree is defined by the quotient $S_M^{coresand} : S_M^{rawsand}$. Any presence of agglomerated sand particles results in a de-agglomeration degree < 1.

To assess time dependency, an identified minimum core removal rate R_{min} is linked with the created specific surface results in the de-agglomeration rate R_S (Eq. (6)).

$$R_S = R_{min}.S_M^{coresand}$$

This criterion reflects the rate at which sand particle bonds are broken up. The de-agglomeration rate predominantly refers to the sand core bonding strength properties. Any pre-damage to the core is reflected (e.g. by different thermal loads or casting contraction stresses), along with the residual core strength and brittleness.

Based upon the measured grain size analysis and the retained mass fraction, all mesh sizes have been obtained. Subsequently, the optimum RRSB distribution was evaluated. Fig. 10 illustrates the variance plot over the field of RRSB parameters that serves to find the optimum RRSB parameter combination for the silica raw sand.

A pronounced minimum is present, with d_p = 0,331 mm and k = 4,178 and a minimum standard deviation $\sqrt{s^2}$ = 1,68%. Standard deviation was below 2 % for all evaluated particle size distribution curves. The measured and modelled retained mass fraction results for the raw sand are documented in Table 2.

RRSB particle size distribution curves for raw sand and the removed core sand of all thermal exposure variants are shown in Fig. 11.

The removed core sand generally shows a shift towards higher particle sizes, indicating the presence of sand agglomerates. The highest lump mass fraction (above 50 %) was found for the hardened condition, followed by the insulated and air-cooled cases. Interestingly, the lump mass fraction was very low for the water-cooled case.

3.3. De-agglomeration behaviour

In Table 3, all results are summarised, while a graphical summary of the de-agglomeration properties of all samples is shown in Fig. 12. The degree of de-agglomeration for the different thermal sample conditions occurs in a typical range for each thermal exposure.

The data reveal that the de-agglomeration rate is direct proportional to the minimum shake-out mass rate and de-agglomeration degree is

Table 3
Shake-out results of all tested samples. The shake-out mass rate, RRSB parameters, evaluated diameter, de-agglomeration degree, and evaluated de-agglomeration rate are documented.

Condition	sample #	Particle size distribution parameters for RRSB fit		Shake-out quarter mass rate R_{25} in gs^{-1}	De-agg.- rate R_S/ $mm^2\,s^{-1}$	Lump mass fraction m_L in %	De-agg.- degree in %
		Grain size parameter d' in mm	Distribution parameter k				
pure	H32	0,331	4,178	–	–	–	100
Hardened	59	0,412	3,986	0,15	481	50	41
	60	0,394	3,781	0,14	460	52	41
	61	0,386	3,661	0,12	426	49	45
Water	50	0,429	5,609	0,21	1236	2	72
	51	0,415	5,175	0,06	343	2	76
	52	0,421	5,344	0,77	4594	2	74
Air	56	0,417	4,075	1,08	4779	31	55
	57	0,421	4,037	4,16	19008	29	57
	58	0,426	4,328	1,94	9292	23	59
Air + open	75	0,431	4,603	1,13	5390	22	59
	76	0,421	4,405	2,29	10681	26	58
Air + Dry	79	0,427	4,689	4,63	23082	19	62
	82	0,416	4,182	5,30	25080	26	59
	83	0,427	4,207	4,70	21796	26	57
Insulation	53	0,414	4,287	1,05	4221	38	50
	54	0,409	4,196	1,99	8091	38	50
	55	0,398	4,166	1,75	6605	44	47

inversely proportional to the lump mass fraction. Thus, applied for quality control purposes these primarily measured characteristics can be evaluated without full grain size analysis already.

The lowest de-agglomeration rate and –degree were observed for the hardened condition. The initial core strength is non-deteriorated by any overlaid loading.

The cast-in samples all exhibited a higher de-agglomeration rate. As previously discussed, this rate was potentially decreased by the influence of ambient air humidity, as different examples with air-cooled samples clearly show. Interestingly, for a longer thermal exposure time (e.g. during insulated cooling), a lower degree of de-agglomeration and higher de-agglomeration rate were found, relative to the water-cooled condition. This may be attributed to thermally induced sand core damage, which can cause binder embrittlement by de-hydration and micro-cracking caused by sand grain expansion.

The major process difference between the externally hardened sample and cast-in and water-cooled samples is the missing casting-core interaction for the hardened sample. This led to the early release of large core lump pieces, and the consequent observed low degree of de-agglomeration. In contrast, the core in the water-cooled sample suffered only minor damage during the casting process, but may have been intensively exposed to hydrostatic pressure from the rapidly contracting quenched casting as the core expanded, because of the low thermal conductivity of the core. These thermomechanical stress conditions could have prevented the early release of the cast-in core during the vibration-induced core removal process.

4. Conclusions

- Sand core disintegration at core removal from cast parts was quantified with a de-agglomeration rate criterion. Two main elements required are the minimum core removal mass rate, which is reflecting the kinetics, and the specific surface area of the removed core sand compared to the initial one of the raw sand.
- The core lump mass constituted a significant fraction of the removed cores sand. The observed core lump disintegration was depending on the casting parameters.
- Particle size measurement of the removed core sand required specifically adjusted parameters. The resulting size distribution was modelled with good accuracy using an approach adopted from the field of mineral processing. This allowed the subsequent calculation of the specific surface area.
- The de-agglomeration rate of non-cast in reference core samples was the lowest. Cast-in cores show higher de-agglomeration rate with increased thermal exposure. Specifically, samples stored without ambient air exchange exhibited the highest de-agglomeration rate.
- Implementation of the method is possible for whichever casting geometry and core removal technology. For intricately shaped cores a complex transient process load overlay could be hindering to access the exact kinetics in experiments. Modelling of local core properties influenced the thermal and mechanical interaction with the cast part might be required.

Acknowledgements

The support from company Nemak Linz for this study by enabling the extensive use of production and engineering facilities is highly acknowledged.

References

Bayat, H., Rastgo, M., Zadeh, M. Mansouri, Vereecken, H., 2015. Particle size distribution models, their characteristics and fitting capability. J. Hydrol. 529, 872–889. http://dx.doi.org/10.1016/j.jhydrol.2015.08.067.

Brown, W.K., Wohletz, K.H., 1995. Derivation of the Weibull distribution based on physical principles and its connection to the Rossin-Rammler and lognormal distributions. J. Appl. Phys. 78, 2758–2763. http://dx.doi.org/10.1063/1.360073.

Czerwinski, F., Mir, M., Kasprzak, W., 2015. Application of cores and binders in metalcasting. Int. J. Cast Met. Res. 28, 129–139. http://dx.doi.org/10.1179/1743133614Y.0000000140.

Fennell, T., Crandell, G., 2008. Inorganic Binder Properties Study. 1413–145 NA.

Principles of Mineral Processing. In: Fuerstenau, M.C., Han, K.N. (Eds.), Society for Mining, Metallurgy, and Exploration, Inc. (SME) (Littleton, Colorado, USA 80127).

Gamisch, M., 2002. Mechanisches Entkernen von Al-Gussteilen mit geringer Beanspruchung des Gussteils. Giesserei-Rundschau 49, 43–45.

Henry (Ashland), C., Showman (Ashland), R., Wandtke (Ashland), G., 1999. Core and foundry process variables affecting aluminum casting shakeout of cold box cores. Trans. Am. Foundry Soc. 107, 99–115.

ISO, 2016. 3310-1:2016-08 2016–08 (E) Test Sieves – Technical Requirements and Testing – Part 1: Test Sieves of Metal Wire Cloth Standard. Beuth Verlag GmbH.

Izdebska-Szanda, I., Angrecki, M., Matuszewski, S., 2012. Investigating of the knocking out properties of moulding sands with new inorganic binders used for castings of non-ferrous metal alloys in comparison with the previously used. Arch. Foundry Eng. 12, 117–120.

Major-Gabryś, K., Dobosz, S.M., Jelinek, P., Jakubski, J., Beno, J., 2014. The measurement of high-temperature expansion as the standard of estimation the knock-out properties of moulding sands with hydrated sodium silicate. Arch. Metall. Mater. 59, 739–742. http://dx.doi.org/10.2478/amm-2014-0123.

PN-85/H-11005, 1985. Moulding and Core Sands Technological Knockout Properties Test (No. PN-85/H-11005). Polish Standards Institute – Polski Komitet Normalizacji, Miar I Jakosci, Poland.

Paluszny, A., Tang, X., Nejati, M., Zimmerman, R.W., 2016. A direct fragmentation method with Weibull function distribution of sizes based on finite- and discrete element simulations. Int. J. Solids Struct. 80, 38–51. http://dx.doi.org/10.1016/j.ijsolstr.2015.10.019.

Quarzwerke, 2009. Quarzsand Haltern H 31 bis H 35, Quarzwerke Stoffdaten. (D-50207 Frechen).

Rosin, P.O., Rammler, E.J., 1933. The Laws Governing the Fitness of Powdered Coal.

Weibull, W., 1951. A statistical distribution function of wide applicability. J. Appl. Mech. 8491543.

Zogg, M., 1993. In: Teubner, B.G. (Ed.), Einführung in die mechanische Verfahrenstechnik, 3rd ed. Burgdorf, Stuttgart.